Title
Optical Measurements of Soot Size and Number Density in a Spray-Atomized, Swirl-Stabilized Combustor

Journal
Journal of Engineering for Gas Turbines and Power, 107(1)

ISSN
0742-4795

Authors
Wood, CP
Samuelsen, GS

Publication Date
1985

DOI
10.1115/1.3239695

Optical Measurements of Soot Size and Number Density in a Spray-Atomized, Swirl-Stabilized Combustor

C. P. Wood
Staff Research Associate.

G. S. Samuelsen
Professor of Mechanical Engineering.

UCI Combustion Laboratory,
Mechanical Engineering,
University of California,
Irvine, Calif. 92717

In-flame optical measurements of soot particulates in a turbulent, recirculating (i.e., complex flow) model laboratory combustor are described. A nonintrusive optical probe based on large-angle (60 and 20 deg) intensity ratio scattering was used to yield a point measurement of soot particulate in the size range of 0.08 to 0.38 μm. A shale-derived JP-8 stock, isooctane, and mixtures of isooctane with various ring and aromatic compounds blended to yield the smoke point of the JP-8 stock were separately injected as a liquid spray through a twin-fluid atomizer. One blend was also introduced prevaporized through a hollow-cone nozzle. The addition of ring compounds to the base isooctane as well as operation on JP-8 increased the amount of soot produced, although the total amount of soot produced depended on fuel type for those fuels of equivalent smoke point. The spatial distribution of soot as well as the amount produced was found to be sensitive to nozzle atomization quality and injection momentum. The amount of soot produced was reduced by a reduction in fuel loading. However, injection of fuel in a prevaporized state both increased the amount of soot produced and changed spatially the region over which soot was distributed. Scanning electron micrographs of extracted samples established that the optical technique resolved the large particle wing of the soot size distribution.

Introduction

Fuel flexibility is a viable and realistic approach to assure adequate availability of aviation fuel through this century. To achieve this position, the relationship of fuel properties and composition to combustion hardware performance and durability must be identified more precisely. Such information is necessary if fuel specifications are to be successfully relaxed to a level that both maintains the required performance of the combustion system (and other subsystems) and permits the desired latitude in the portion of hydrocarbon resources (petroleum, oil shale, coal, tar sands, etc.) that can be utilized to produce aviation fuel. These potential changes in fuel processing and fuel source make future fuel composition effects on gas turbines a primary consideration and concern.

Currently, the specification limit on aromatics for aviation fuel is a maximum of 20 percent (Jet A) or 25 percent (JP-4, JP-5, JP-8) by volume. The limit is set to preclude a series of combustion-related problems associated with the production of soot, examples of which include increased flame radiation, deposit of carbonaceous material, and emission of particles. Radiation and deposition influence hardware durability and performance, while the emission of particles results in aesthetic and tactical problems. The aromatic content is of special interest because a relaxed specification for aromatics could ease the demand for hydrogen addition in the refining of low hydrogen resources. An upper limit of 35 percent aromatics has been discussed [1].

To accommodate an increased fuel aromaticity, the production of soot from combustors operating on relaxed-specification fuels must be reduced. Toward this end, experimental evidence is needed with respect to the effects that fuel properties, fuel-additive properties, and combustor operating conditions have on soot formation and burnout. Of particular interest are the mass emission, size distribution, and composition of the soot particulate. Extractive probe measurements have been used in the past to derive this set of information (e.g., [2, 3, and 4]) but, in complex flows where backmixing can exacerbate and widely distribute perturbations introduced by the presence of a physical probe, caution must be exercised in the use of such methods [5]. This may include limiting the measurements to the combustor exit-plane, far downstream of the recirculation zone. Such a limit substantially restricts the information available. Excluded is the spatial distribution of local soot size and soot number

Contributed by the Gas Turbine Division of The American Society of Mechanical Engineers and presented at the 29th International Gas Turbine Conference and Exhibit, Amsterdam, The Netherlands, June 4–7, 1984. Manuscript received at ASME Headquarters January 9, 1984. Paper No. 84-GT-153.

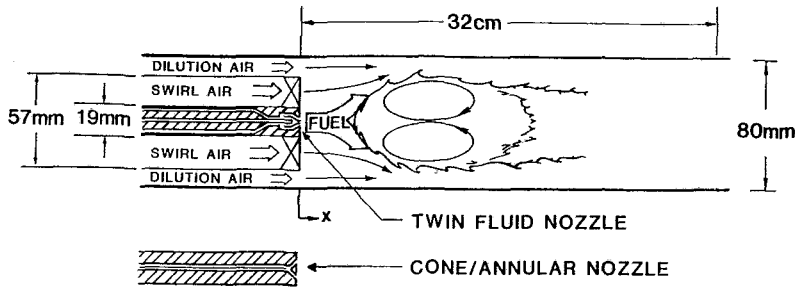

Fig. 1 Dilute swirl combustor

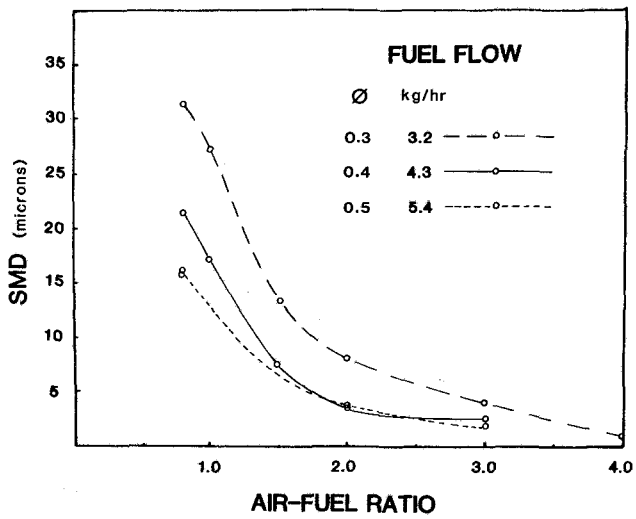

Fig. 2 Nozzle characterization

density in the near wake of the recirculation zone and within the recirculation zone itself. Such measurements must be nonintrusive and therefore rely on optical techniques. Although optical techniques have been successfully employed to measure soot in relatively simple flows (flat flames and diffusion flames), limited applications to complex flows have only recently been demonstrated [5, 6].

In a recent study [6], we addressed the application of a nonintrusive, optical probe to a complex flow where the principal objective was to evaluate the performance of large angle intensity ratioing for optically measuring the local soot size and soot number density in the reaction zones of a complex flow. Isooctane and blends of isooctane with pure hydrocarbons of varying aromaticity were introduced prevaporized. In the present study, the objectives were to (*i*) introduce the fuels as liquid sprays and add to the fuels tested a shale-derived JP-8, and (*ii*) conduct an exploratory assessment of the impact of key parameters (fuel molecular structure, atomization quality, injection state) on the spatial distribution of soot in a model laboratory complex flow combustor.

Experiment

(a) Approach. The approach was to optically measure the spatial distribution of local soot size and number density in a model laboratory complex flow combustor. Radial profiles were measured at three axial locations for a shale-derived JP-8, isooctane, and three fuel blends introduced through a twin-fluid atomizer. The three fuel blends were mixed to yield the same ASTM smoke point as the JP-8 in order to assess the effect of fuel molecular structure on soot yield in a complex flow. The effect of atomization quality was addressed for the shale-derived JP-8, and a parametric variation was conducted on one fuel blend to assess the effect of injection state (prevaporized versus liquid fuel injection) on soot yield. The optical technique employed was scattering intensity ratioing at two angles, 60 and 20 deg.

(b) Combustor. The combustor employed was a model laboratory complex flow combustor developed in a series of tests [7, 8]. The configuration is presented in Fig. 1. The Dilute Swirl Combustor (DSC) features an aerodynamically controlled, swirl-stabilized recirculation zone to simulate important features of practical combustors (e.g., swirl and highly turbulent recirculation).

For the present work, the housing consisted of an 80-mm-i.d. cylindrical stainless steel tube that extended 32 cm from the plane of the nozzle. Rectangular, flat windows (25 × 306 mm) were mounted perpendicular to the horizontal plane on both sides of the combustor tube to provide a clear, optical access for the laser measurements.

A set of swirl vanes (57-mm-o.d.) were concentrically located within the tube around a 19-mm-o.d. centrally positioned fuel delivery tube. Dilution and swirl air were metered separately. The dilution air was introduced through flow straighteners in the outer annulus. The swirl air passed through swirl vanes with 100 percent blockage, which imparted an angle of turn to the flow of 60 deg. For the swirl-to-dilution air flow ratio of 1.66 used in the present study, the swirl number obtained by integrating across the swirl vanes was 1.3; that obtained by integrating the total inlet mass flux was 0.5. Prototype 60 deg swirl vanes with a 70 percent blockage, used in the initial study for prevaporized fuel injection [6], were not adequate for the liquid injection. Higher blockage provides a wider range of stable operation for the liquid injected fuels.

Fuel was introduced through a twin-fluid injector designed for the present study by Parker-Hannifin. Sauter Mean Diameter (SMD) was measured using a Malvern ST2200 laser diffraction instrument as a function of nozzle air-to-fuel mass ratio and compared to data generated by Parker-Hannifin [9]. The data are presented in Fig. 2. Although the values of SMD approach the limit of resolution for the Malvern as nozzle air-to-fuel ratio is increased, the trend toward enhanced atomization quality is clearly evident. The intensity ratioing results of the present work were obtained for an air-to-fuel mass ratio of 3.0. For the shale-derived JP-8, data were also obtained at air-to-fuel ratios of 2.5 and 3.5 to assess the effect of this parameter on soot size and spatial distribution. A cone-annular nozzle was used for the one fuel blend introduced in a prevaporized state.

The combustor was operated at atmospheric pressure to provide for the necessary optical access and ease of operation with the relatively complex and unhardened optical system employed. The effect of pressure, an important parameter in the production of soot, is appropriate for evaluation once the utility and applicability of the optical system is established and adaptability of elevated pressure systems to optical access is demonstrated.

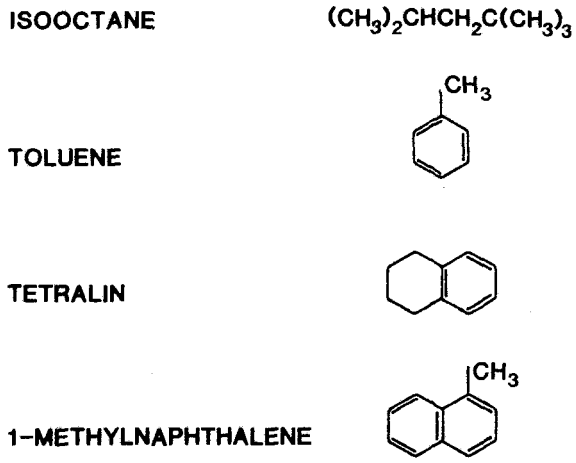

Fig. 3 Fuel molecular structure

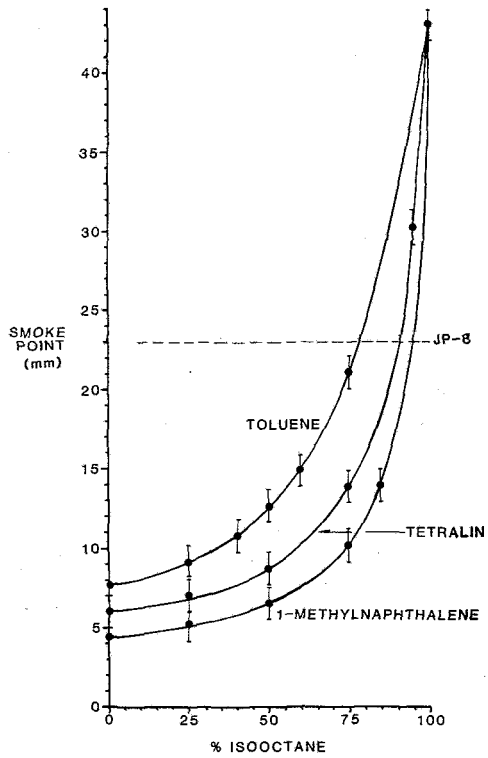

Fig. 4 ASTM smoke point

(c) **Fuels.** A shale-derived JP-8 and four liquid fuels of varying molecular structure representative of compounds found in petroleum, shale, and coal-derived fuels were used in this study. Isooctane (2, 2, 4-trimethylpentane) served as the base fuel as it represents a major component of JP-8 and serves as the reference fuel in the ASTM smoke point test. The three remaining fuels consisted of mixtures of isooctane with one of three compounds with varying degrees of saturation and ring number (Fig. 3)—toluene, tetralin (1, 2, 3, 4-tetrahydronaphthalene), or 1-methylnaphthalene.

The amount of hydrocarbon blended with the isooctane was selected to yield the same ASTM smoke point as that obtained for the JP-8 stock. The amount of each compound blended with isooctane was determined by first preparing a curve of smoke point versus volume percent isooctane (Fig. 4). Table 1 summarizes the composition and the actual smoke point found for each blend. The smoke points, while not identical, are equivalent within the achievable accuracy of the smoke point test (± 1 mm) shown by the error bands in Fig. 4.

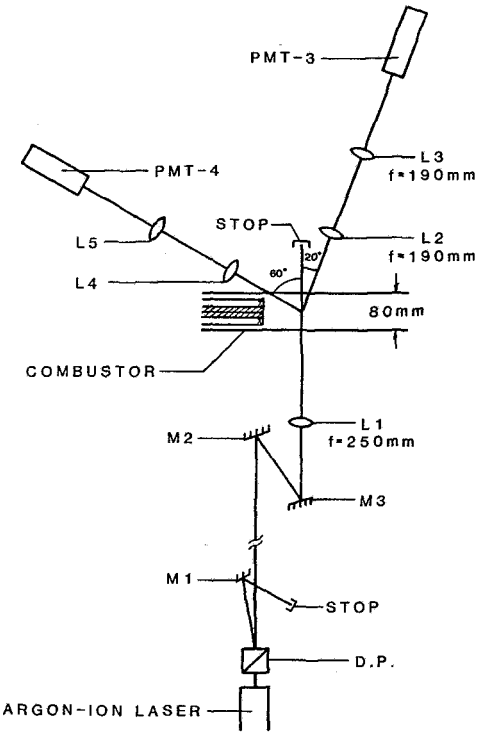

Fig. 5 Optical configuration

Table 1 Fuel summary

Fuel[a]	Smoke point[b]	H wt. %
Isooctane	43.0	15.79
JP-8	23.0	13.89[c]
Blend 1 21% toluene/ 79% isooctane	24.0	14.02
Blend 2 8% tetralin/ 92% isooctane	25.3	15.06
Blend 3 5% 1-methylnaphthalene/ 95% isooctane	22.2	15.16

[a] Blend composition stated in volume percent
[b] Distance above base of burner in mm at which sooting first occurs
[c] Wright Patterson AFB
Source: [4]

(d) **Optical System.** The method adopted for the point-measurement of particle size and number density of soot particulate was scattering intensity ratioing. Figure 5 illustrates the optical configuration, a modification of that used previously [5]. This earlier work utilized collection optics at 10 and 5 deg off the optical axis. The current work employed collection optics at 60 and 20 deg to reduce the smallest size of particles that could be resolved from 0.3 to 0.08 μm.

A 5-watt Model 165 Spectra-Physics argon-ion laser operating in the multiline mode was used as the source of light. The laser lines were separated by a dispersion prism to resolve the blue line (488.0 nm). The beam was focused to a 110 μm waist dia using a 50-mm-dia F/5 focusing lens. The scattered intensity was detected at 60 and 20 deg which provided a particle size detection band of $0.08\ \mu m < d < 0.38\ \mu m$. Other angles were available but 60 deg/20 deg provided the smallest resolvable size (0.08 μm) of those pairs available.

The scattered light was focused to two photomultiplier tubes (RCA Model 8575) having quantum efficiencies of

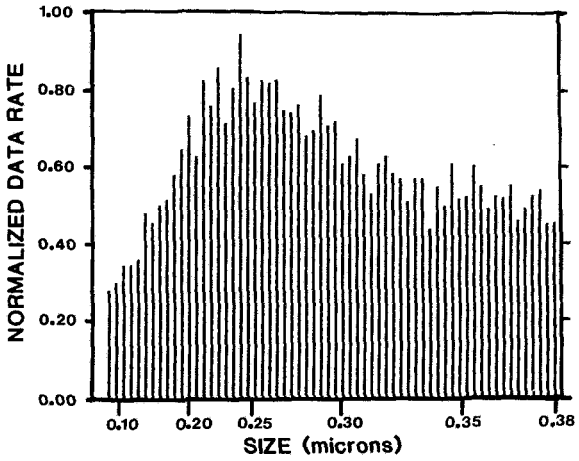

DATE: 21SEP83
SERIES: ISOTET RUN: 1006 21SEP83
COMMENT: D=DATA HV=1200/1220 LASER=1W
R/R=0.83 X/R=3.0 EQ/R=0.5 V=7.5M/S

MAX RAW COUNT = 764
TOTAL RAW COUNT = 30131
SAMPLE TIME: 11.4 SECONDS

LISTING OF RAW COUNTS

RATIO	BIN COUNT	RATIO	BIN COUNT
.946	225	.31	584
.913	239	.299	492
.881	278	.289	508
.85	279	.278	545
.82	285	.268	467
.791	387	.259	429
.763	367	.25	492
.736	405	.241	506
.71	418	.232	472
.685	472	.224	459
.661	522	.216	410
.637	594	.209	461
.615	506	.201	458
.593	670	.194	352
.572	615	.187	442
.552	696	.181	398
.532	575	.174	491
.513	652	.168	414
.495	764	.162	421
.478	672	.156	487
.461	620	.151	445
.444	669	.145	393
.429	665	.14	423
.414	669	.135	418
.399	605	.13	443
.385	597	.126	369
.371	616	.121	393
.358	549	.117	419
.345	563	.113	433
.333	634	.109	362
.321	573	.105	364

Fig. 6 Representative optical data (isooctane/tetralin, $\phi = 0.5$, $r/R = 0.83$, $x/R = 3.0$)

approximately 15 percent at the 488.0 nm wavelength with pinhole aperature diameters of 200 μm. The supply voltage to the tubes was approximately 1200 V.

The output signal from the photomultiplier tubes was passed into a Spectron Development Laboratories (SDL) Model LA-1000 logarithmic amplifier, which converted the negative current to a positive voltage and was scaled for +10 V peak output when the input current was −1 mA. The amplified signals were then fed to a SDL Model RP-1001 Intensity Ratio Processor (RP). The RP registered and processed the peaks of the two signals provided certain criteria were met. The d-c voltages input from the two channels of the logarithmic amplifier were processed by an analog subtractor circuit in the RP, which amplified the signal

Table 2 Test matrix

Fuel[a]	Overall equivalence ratio ϕ	Nozzle air-to fuel ratio	Injection state	Fig.
Isooctane	0.3,0.5	3.0	liquid	9
JP-8	0.3	2.5,3.0,3.5	liquid	10
Blend 1- 21% toluene/ 79% isooctane	0.3,0.5	3.0	liquid	9
Blend 2- 8% tetralin/ 92% isooctane	0.3,0.5 0.3,0.5	3.0 NA[b]	liquid prevap.	9 9,11
Blend 3- 5% 1-methyl-naphthalene/ 95% isooctane	0.3,0.5	3.0	liquid	7,9

[a] Blend composition stated as volume percent
[b] NA = not applicable

with a gain of 5 and converted the signal to an 8-bit binary number. The RP had a variable lower threshold voltage, allowing a measure of control over the rejection of background noise.

The binary output was fed to an Apple II microcomputer, which resolved this output into 62 bins. The size distribution was determined by the number of counts in each bin, where each bin encompassed a discrete size range. The counts in each bin were then divided by the time required to collect them, resulting in a count rate (counts/s). A histogram was then generated of normalized data rate versus size (in microns). The normalization of this histogram was under the operator's control through the system software. The histogram could be normalized to itself (giving the bin with the highest sooting rate an intensity of 1.0); it could be normalized to the highest sooting rate among all the histograms generated for a particular fuel; or it could be normalized to the highest sooting rate among any number of fuels or operating conditions. The results of this normalization procedure are evident in Figs. 7, 9, 10, and 11.

The interpretation of the measured intensity ratio is based on the analysis of the Mie scattering properties of a homogeneous, isotropic spherical particle. Soot, a nonspherical scatterer with an index of refraction of some uncertainty, therefore requires special consideration. An evaluation of such effects, considered in an earlier study, concluded that the combined error was 20–30 percent with some broadening of the distribution [5].

Calibration of the optical system was performed routinely at the beginning of each run session using polystyrene particles of a known size (mean diameter = 0.255 μm, standard deviation = 0.9 percent). Calibrations were regularly checked as well at the end of each run session to verify that the optical quality of the combustor windows had not degraded. In addition, consistency in the performance of the combustor and optical system was monitored over a period of weeks by periodically repeating the isooctane/tetralin data set. After attaining thermal equilibrium, nine points in the flow field were monitored for soot data rate and size distribution. At any given station, the variation in the peak of the size distribution of the soot never exceeded 10 percent of the nominal value at that station. The data rate was more variable. Along the outer perimeter of the combustor (e.g., $r/R = 0.83$), where nominal sooting rates exceeded 1500 Hz, the variation in data rate was approximately 30 percent. At the interior stations, where sooting rates were nominally below 300 Hz, the data rate varied from 47 to 71 percent, depending on the station, with the greater variability correlated with lower data rate. The variability of the data rates is not unreasonable at this point in the system

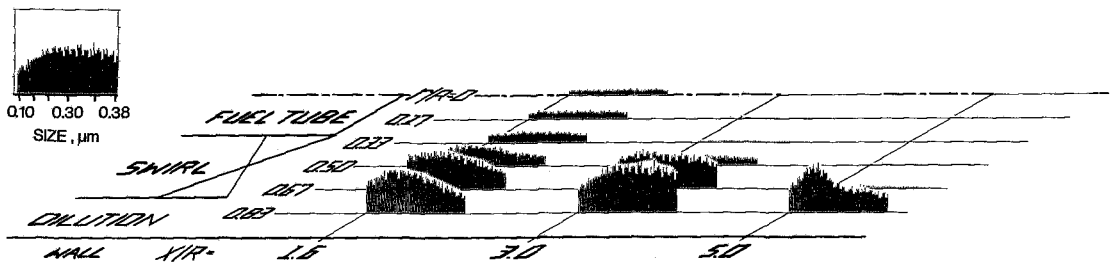

Fig. 7 Spatial map (isooctane/1-methylnaphthalene, $\phi = 0.5$)

Table 3 Data rate (Hz)

Fuel	Equivalence ratio ϕ	Location							Injection state	Fig.
		Axial x/R	Radial r/R							
			0	0.17	0.33	0.50	0.67	0.83		
Isooctane	0.5	1.6	57	70	66	61	109	247	liquid	9(*a*)
		3.0	0	0	0	0	7	26		
		5.0	0	0	0	0	0	1		
Blend 1	0.5	1.6	30	72	122	204	406	581	liquid	9(*b*)
21% toluene/		3.0	0	0	1	6	65	296		
79% isooctane		5.0	0	0	0	4	59	419		
Blend 2	0.5	1.6	236	305	389	700	1521	1982	liquid	6,9(*c*),11(*c*)
8% tetralin/		3.0	1	6	61	444	1775	2643		
92% isooctane		5.0	0	1	3	9	98	1746		
Blade 3	0.5	1.6	260	346	450	770	1482	1612	liquid	7,9(*d*)
5% 1-methylnaphthalene/		3.0	0	5	61	429	1532	1991		
95% isooctane		5.0	0	1	2	6	90	1399		
JP-8	0.3	1.6	26	25	24	22	24	21	liquid	10(*a*)
(A/F = 3.0)		3.0	22	22	20	14	12	19		
		5.0	105	134	122	25	10	15		
JP-8	0.3	1.6	45	46	53	61	42	20	liquid	10(*b*)
(A/F= 2.5)		3.0	425	330	311	166	29	28		
		5.0	1812	1686	1211	470	88	20		
JP-8	0.3	1.6	13	10	11	35	236	372	liquid	10(*c*)
(A/F= 3.5)		3.0	11	11	10	12	56	269		
		5.0	6	8	10	24	92	191		
Blend 2	0.5	1.6	1505	1221	874	468	142	103	prevaporized	11(*a*)
8% tetralin/		3.0	1054	775	928	373	143	244		
92% isooctane		5.0	183	394	1761	934	861	3373		
Blend 2	0.3	1.6	1120	980	857	603	239	239	prevaporized	11(*b*)
8% tetralin/		3.0	313	345	887	416	282	488		
92% isooctane		5.0	284	677	2364	1023	1914	3816		
Blend 2	0.5	2.3	1200	1590	1347	1175	1631	2236	prevaporized	11(*d*)
8% tetralin/		3.7	1269	1293	1717	2104	2361	2708	(weak swirl)	
92% isooctane		5.0	1164	1081	1291	1686	2032	2405		

development. Several parameters of the measurement system can influence the rate, including the alignment and focusing of two optical detectors at a coincident point and the signal processor thresholds. In addition, the condition of the twin-fluid injector was found to have a marked effect on data rate. The specific orientation of the injector with respect to the combustor flow field was found to change the sooting rate at specific points in the flow field, presumably because of resulting changes in fuel distribution caused by small asymmetries in the atomized spray. The effect of nozzle configuration and performance on fuel distribution and soot production is an area of active interest and will be explored in more detail in future work.

(e) Test Matrix. The test matrix for the present study is presented in Table 2. Tests were conducted at overall equivalence ratios of 0.3 and 0.5, except for the JP-8, which was tested only at 0.3. (At equivalence ratios greater than 0.3, a portion of the atomized JP-8 was found to penetrate the recirculation zone and impinge on the walls of the combustor). The nominal air-to-fuel rate for the nozzle was 3.0 for the JP-8, isooctane, and three blends. The nozzle air was in addition to the main air (swirl plus dilution) and corresponded to 10 and 6 percent of the main air at $\phi = 0.5$ and $\phi = 0.3$, respectively. Although not optimum for each individual case, an air-to-fuel ratio of 3.0 was selected as the operating condition that provided the most satisfactory

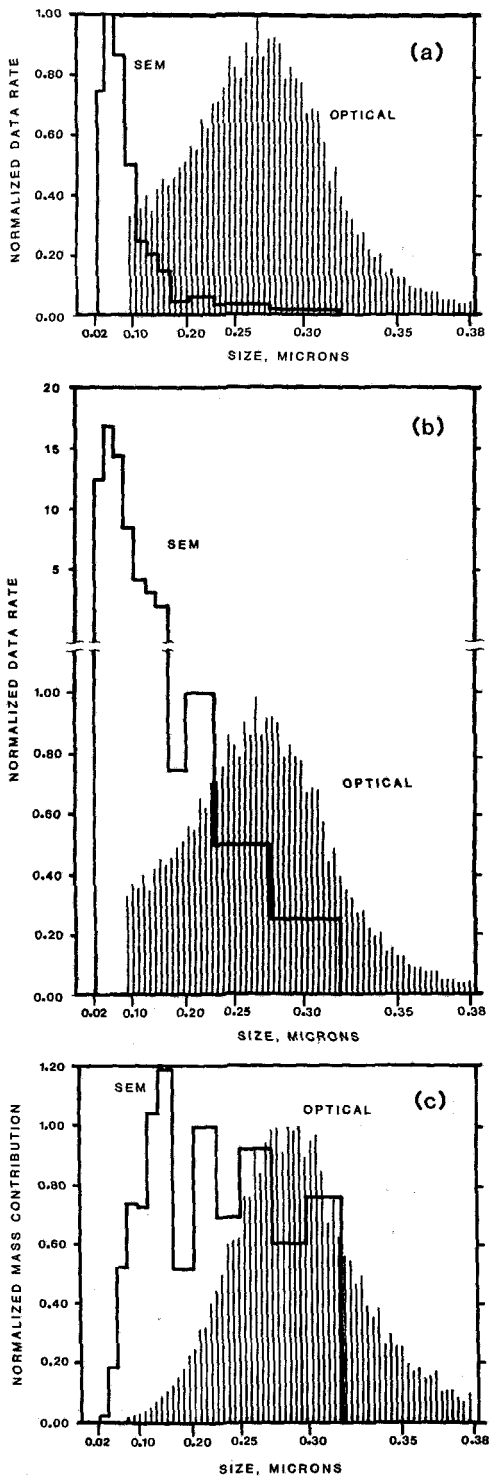

Fig. 8 Validation [6] (isooctane/toluene, ϕ = 0.5, prevaporized): (a) number density; (b) number density renormalized; (c) mass density

performance (highest stability) for the group of fuels tested. The effect of atomization quality was demonstrated for the shale-derived JP-8. The combustor was operated at a reference velocity of 7.5 m/s.

Results

The results are presented in two groups. The performance and utility of the optical system for in-situ, nonintrusive measurements of soot size and number density are first evaluated. Second, the effects of fuel molecular structure, fuel loading, nozzle performance, and injection state on the spatial variation of soot size and number density within the combustor are assessed.

(a) Data Presentation. An example of the data provided by the optical system is shown in Fig. 6 for the tetralin blend at ϕ = 0.5. The histogram represents the distribution of intensity ratio for 30131 validated samples. The total data rate for this case (2643 Hz) is the number of validated samples (30131) divided by the total sample time (11.4 s) and represents the sum of the bin data rates for each of the 62 bins comprising the histogram. The total data rate for each sampling location for this case and for all fuels and conditions tested is listed in Table 3.

The utility of a point measurement is the ability to map the combustor for soot size and number density. An example of such a mapping is presented in Fig. 7 for the 1-methylnaphthalene blend at ϕ = 0.5. Radial profiles of optically measured soot size and number density are presented at three axial locations within the combustor. The locations of peak soot concentration for the 1-methylnaphthalene blend can be identified (x/R = 1.6; r/R = 0.83), and the reduction of soot downstream is clearly evident.

The effects of fuel molecular structure, nozzle performance, and injection state on the soot field are presented in Figs. 9, 10, and 11, respectively. In Fig. 7, as well as in Figs. 9, 10, and 11, radial and axial locations are nondimensionalized to the combustor radius (R = 40 mm). All the histograms in Figs. 7, 9, and 10 represent results obtained with the fuels injected as liquids and are, as a result, normalized as a group to the peak bin data rate in the set (JP-8, Fig. 10(*b*)). In Fig. 11, the state of fuel injection is varied. Hence these histograms are normalized to the peak bin data rate in this set (prevaporized isooctane/tetralin, Fig. 11(*b*)). To assist in comparing the histograms in each three-dimensional plot and within each set of results, the histogram with the peak bin data rate in the field is reproduced and dimensioned in the upper left corner of each plot. Because the peak bin data rate in Fig. 7, for example, is normalized to the peak bin data rate of JP-8 in Fig. 10(*b*), the height of the histogram in the upper left corner of Fig. 7 is less than unity.

(b) Evaluation. To validate the optical system, the optical probe was positioned at the entrance of an extractive probe used previously [5]. The extractive probe was located at an axial location (x/R = 5.0) and radial location (r/R = 0.83) well displaced from the centerline where flow perturbation was expected to be minimized. A scanning electron microscopy analysis of the extracted sample was compared to the optical data. The results, reported previously [6], are summarized here for completeness.

The morphology of the soot is agglomerates of smaller (~0.05 μm) spherical particles, which is consistent with the morphology and size observed in other combustor studies (e.g., [4, 5, 6, 10, 11]). An example of the size distribution derived from a scanning electron micrograph (SEM) of the extracted sample is compared to the optical measurement for an isooctane/toluene blend in Fig. 8(*a*). Particle sizes observed optically are also revealed by the SEM data. However, the range of particle sizes resolved by the 60 deg/20 deg intensity ratioing (*i*) is at the large particle end of the SEM distribution, (*ii*) encompasses only a small portion of the total number of particles, (*iii*) includes the agglomerates, and (*iv*) excludes the primary particles.

Although the optical data do not include the peak size of the actual distribution (~0.05 μm, the size of the primary particles), the optical data appear to accurately reflect a secondary peak located in the large particle wing of the SEM data. To more effectively compare the two sets of data, the

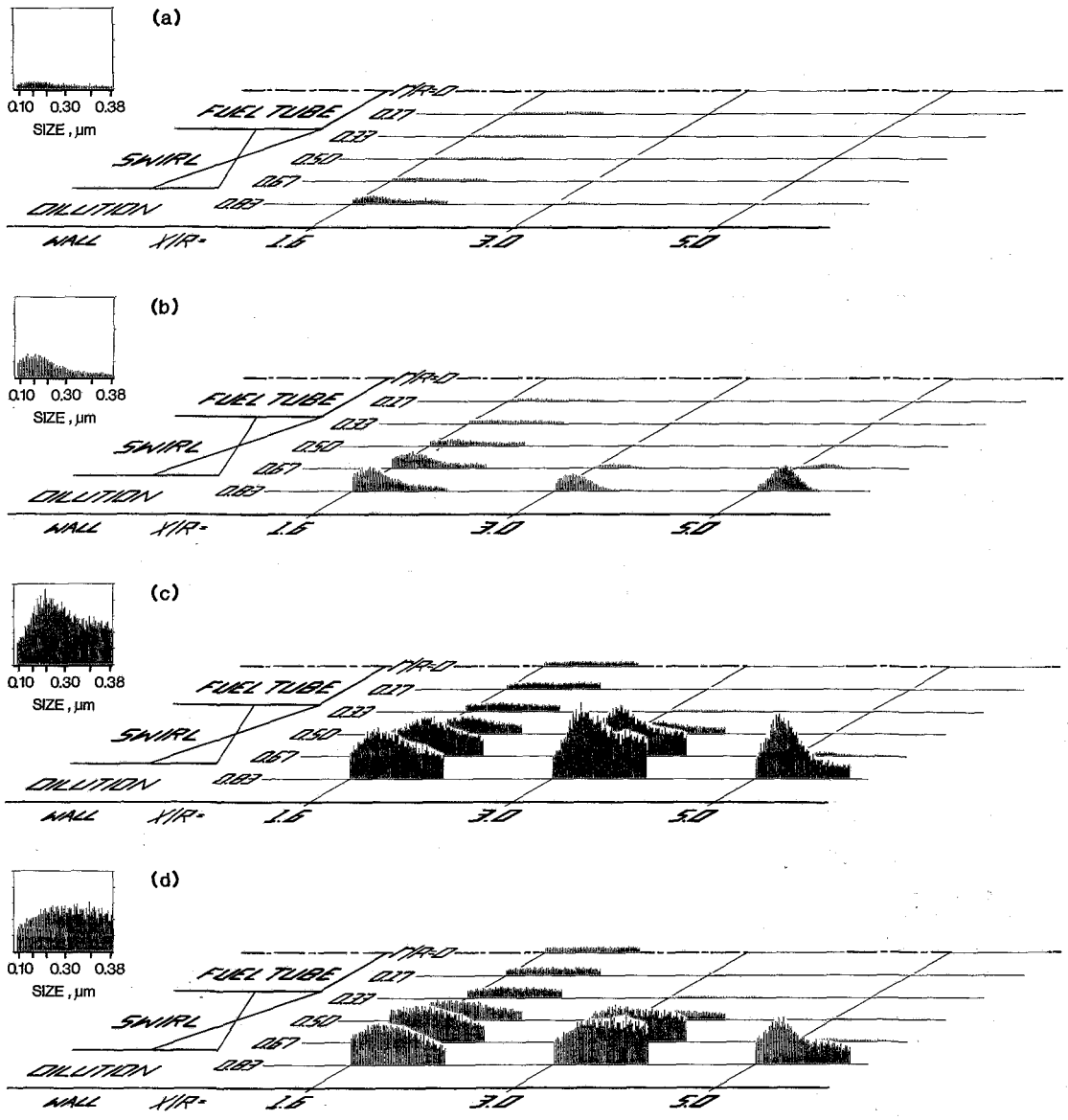

Fig. 9 Fuel molecular structure (ϕ = 0.5): (*a*) isooctane; (*b*) isooctane/toluene; (c) isooctane/tetralin; (*d*) isooctane/1-methylnaphthalene

SEM data are renormalized in Fig. 8(*b*) to the secondary peak in data rate that occurs in the large particle wing of the SEM distribution ($d_p \sim 0.22$ μm). The optically measured peak in data rate appears to be real and reflects a discontinuity in particle size associated with agglomerate growth. However, the extent to which the optically measured data rate is reduced on the small particle side of the peak may be exaggerated due to an inaccuracy in the optical technique associated with the Gaussian intensity profile of the incident laser beam. A relatively small particle passing through the laser beam at the wing of the Gaussian intensity profile may not scatter enough light to the detectors to meet established threshold levels on the RP, whereas a larger particle, passing through the same region of the beam, will scatter enough light to be recorded. This acts to artificially suppress the low end of the distribution. This inaccurcy is amenable to an analytically derived "probe volume" correction which could be implemented through the reduction software, in essence giving the system a flat response throughout the range of sizes it is theoretically capable of measuring. Other sources of inaccuracy are discussed in [6].

In Fig. 8(*c*), both the optical and SEM distributions are presented in terms of mass density. Although the difference in relative peak levels is not as pronounced, it is nonetheless still striking.

(c) Parametric Assessment.

Fuel Molecular Structure. The results for the effect of fuel molecular structure on soot size and number density are presented in Fig. 9 for isooctane and the three blends (79 percent isooctane/21 percent toluene; 92 percent isooctane/8 percent tetralin; 95 percent isooctane/5 percent 1-methylnaphthalene) prepared to yield the same smoke point as a JP-8 stock. The data are normalized to the peak bin data rate observed for JP-8 at an air-to-fuel ratio = 2.5, ϕ = 0.3 (Fig. 10(*b*)). The total data rates for each location are tabulated in Table 3.

It is first noteworthy to compare the results for the isooctane blends (Figs. 9(*b,c,d*)) with the results for the pure isooctane (Fig. 9(*a*)). The data rates for the blends are higher than the data rates observed for the pure isooctane. Hence the addition of ring compounds (as small as 5 percent by volume in the case of 1-methylnaphthalene) has a substantial impact on the soot produced.

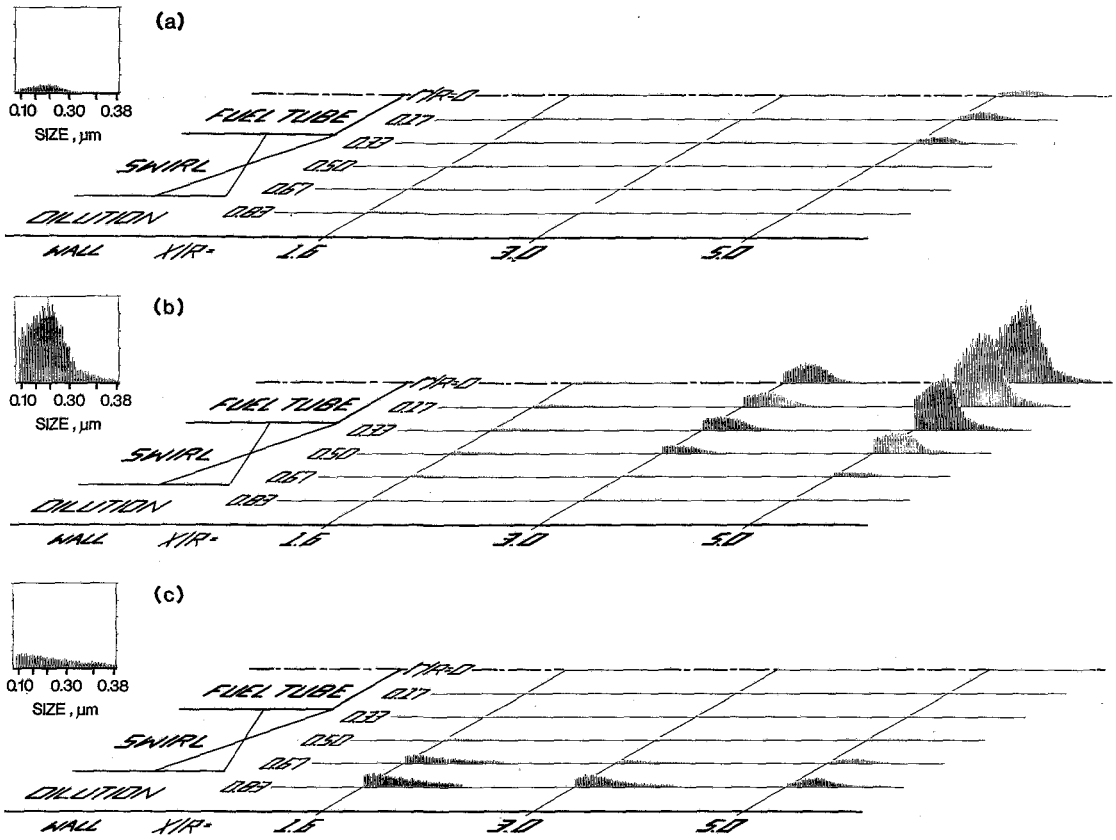

Fig. 10 Nozzle performance (JP-8, $\phi = 0.3$): (a) A/F = 3.0; (b) A/F = 2.5; (c) A/F = 3.5

For the isooctane and all three blends, soot is observed at all radial stations at the $x/R = 1.6$ axial station, but only at the outer radial stations at $x/R = 3.0$ and 5.0. This is attributed to (*i*) the intersection of the $x/R = 1.6$ axial station with the recirculation zone, the outer boundary of which extends to approximately 80 mm ($x/R = 2.0$), and (*ii*) the injection of the fuel into the outer boundary ("shear layer") of the recirculation zone. Note that the data rate is of the same magnitude for radial stations within the recirculation zone ($0 < r/R < 0.50$), which is consistent with the presence of a zone of strong backmixing.

The peak data rate for the isooctane and fuel blends occurs at the outer radial positions, coincident with the injection of fuel into the shear layer. Downstream of the recirculation zone ($x/R = 3.0$, 5.0), the soot particles are transported radially outward as a consequence of the strong swirl.

The data rate for isooctane drops dramatically at the two downstream locations and, at $x/R = 5.0$, the soot particulate is completely burned out. The addition of ring compounds, by contrast, not only results in more soot produced, but shows evidence of only marginal burn out.

The distribution of soot particulate has both similarities and significant differences in this data set. The distributions are similar in the relatively uniform distribution in the recirculation zone. The flatness of the distribution reflects an early stage of particulate formation prior to the onset of agglomerate growth. Evidence for the agglomerate growth is reflected in distributions measured at locations displaced from the recirculation zone, namely at $x/R = 1.6$ ($0.67 \leq r/R \leq 0.83$), $x/R = 3.0$, and $x/R = 5.0$. The distribution differs as to where within the combustor the agglomerate begins to build. The buildup of the agglomerate peak occurs further away from the recirculation zone as the molecular complexity of the ring compound increases. This reflects the longer time for fuel pyrolysis and/or longer time for polymerization as the fuel complexity increases.

Data were also obtained at a reduced fuel loading ($\phi = 0.3$) for the isooctane and three fuel blends. Virtually no soot particulate was detected by the optical probe at any of the eighteen sampling points within the combustor (e.g., total data rates were less than 1 Hz). In direct contrast, the total data rates for the shale-derived JP-8 at $\phi = 0.3$ were not insignificant (Table 3, Fig. 10(*a*)). It is also noteworthy that the highest sooting rate occurs at the centerline for the JP-8. This is attributed to the probable collapse of a portion of the fuel jet onto the centerline at this lower nozzle fuel flow rate. Such a collapse has been detected with two-color anemometry by Brum and Samuelsen [8] and the subsequent centerline formation of soot has been verified with high-speed video recordings.

Finally, the fuel blends, mixed to the same smoke point as the shale-derived JP-8, produced different soot yields (area-weighted soot flux) at the last axial plane sampled ($x/R = 5.0$, Figs. 9(*b–d*)). The double-ring tetralin and 1-methylnaphthalene blends both yielded a higher soot level than the single-ring toluene blend. The tetralin blend yielded the highest production of the three. At $\phi = 0.3$ the JP-8 yielded significant soot, whereas the blends yielded no soot at this lower equivalence ratio.

Nozzle Performance. To assess the effect of nozzle performance, the nozzle air-to-fuel (A/F) ratio for one fuel, the JP-8, was varied from the nominal value of 3.0 by changing the air flowrate at a constant fuel flowrate corresponding to $\phi = 0.3$ (Fig. 10). At a degraded level of performance ($A/F = 2.5$), the soot production went up markedly (Fig. 10(*b*)). This demonstrates the importance of nozzle performance in dictating sooting levels. As further

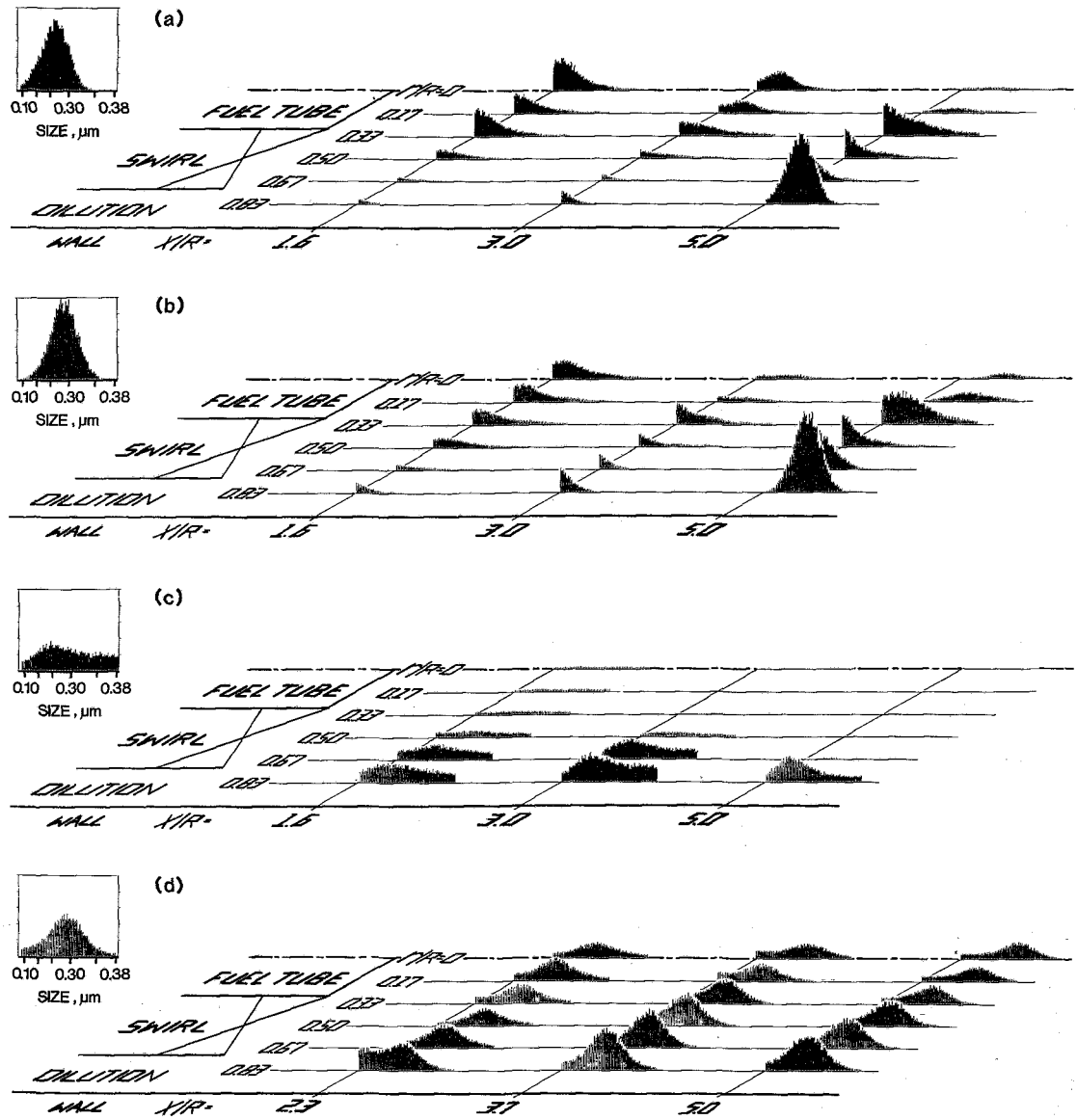

Fig. 11 Injection state (isooctane/tetralin): (*a*) prevaporized injection, $\phi = 0.5$; (*b*) prevaporized injection, $\phi = 0.3$; (*c*) liquid injection, $\phi = 0.5$; (*d*) prevaporized injection, diminished swirl intensity, $\phi = 0.5$

evidence for this, note that the spatial distribution of soot for $A/F = 3.5$ (Fig. 10(*c*)) is different from that measured for $A/F = 3.0$ and 2.5 Figs. 10(*a*,*b*)), and similar to the spatial distributions measured for the blends at $\phi = 0.5$, $A/F = 3.0$ (Figs. 9(*b*,*c*,*d*)). This is attributed to a higher fuel momentum associated with the higher A/F (in the case of the JP-8 at $\phi = 0.3$) and higher fuel flow rate (in the case of the blends at $A/F = 3.0$), thereby preventing collapse of fuel onto the centerline.

Prevaporization. One blend (92 percent isooctane/8 percent tetralin) was injected prevaporized through a cone-annular nozzle (see Fig. 1) to assess the sooting propensity when evaporation of injected droplets is not a factor in the injection and subsequent fuel/air contacting. The results are shown in Fig. 11 for $\phi = 0.5$ (Fig. 11(*a*)) and $\phi = 0.3$ (Fig. 11(*b*)). (The tetralin blend injected in the liquid state at $\phi = 0.5$ is shown in Fig. 11(*c*) and is normalized to Fig. 11(*b*) for comparison.) The soot yield was greater for the fuel injected prevaporized and soot was present at all points measured in the combustor. This is consistent with previous results [6], shown in Fig. 11(*d*), where the swirl was not as intense. This difference in sooting behavior is attributed to the different fuel distribution in the recirculation zone resulting from (*i*) the state of the fuel when injected, and (*ii*) the nozzle. Fuel injected as a vapor enhances the early mixing with the air, and rapidly breaks down the jet penetration. The resulting flames reflects a fuel rich, diffusion type core that extends out of the combustor, giving enhanced sooting levels at the interior radial positions along the entire length of the duct. In contrast, fuel injected as liquid droplets can direct the fuel into the outer boundary of the swirl-induced recirculation zone (the shear layer) resulting in enhanced processing of the fuel within the recirculation zone. This decreases the diffusion type character of the flame, reduces the soot produced, and limits the presence of soot to the outer portion of the combustor.

Summary and Conclusions

An optical system based on large angle intensity ratioing has been used to measure soot particulate in an aerodynamically complex flow field representative of a practical turbine combustor. The utility of such a diagnostic

tool is the provision of detailed mapping to identify the regions of soot formation and burnout. To demonstrate the utility and applicability of the technique, parametric variation on fuel molecular structure, fuel loading, nozzle performance, and injection state were performed. The results are summarized in the following list of observations and conclusions:

Summary of Observations.

- Blends of ring compounds in isooctane (as little as 5 percent 1-methylnaphthalene) produced substantially more soot than the isooctane alone.
- Blends mixed to the same smoke point as a shale-derived JP-8 and injected as liquid sprays yielded less soot than the JP-8 and varied among the blends in the yield of soot with the multi-ring tetralin and 1-methylnaphthalene blends producing substantially more soot than the single-ring toluene blend.
- The soot yield for the blend injected prevaporized was higher than for the fuel injected as a liquid. Whereas soot was virtually absent in the core of the combustor for the blends injected as liquids, the soot was spatially distributed more evenly throughout the combustor for the blend injected prevaporized. This is attributed to the reduced momentum of the prevaporized fuel jet and subsequent collapse of a portion of the fuel onto the centerline.
- Although the shale-derived JP-8 yielded more soot than the blends mixed to the same smoke point, an increased nozzle air-to-fuel ratio substantially reduced the soot produced and indicates that nozzle performance and combustor aerodynamics can be tailored to reduce the soot yield to approximately that of the blends. Nozzle air-to-fuel ratio not only changed the soot yield but also changed the spatial distribution of soot. At low air-to-fuel ratios, both the fuel jet momentum and atomization quality is degraded, a portion of the fuel collapses onto the centerline, and soot is produced in the core of the combustor. At high air-to-fuel ratios, the fuel is injected and processed in the shear layer of the recirculation zone.

Conclusions.

- The spatial distribution of soot, as well as the soot yield in a complex flow combustor, is a function of not only fuel molecular structure and fuel loading, but of flow aerodynamics and pattern of fuel injection. This result points to (*i*) the importance of *aerodynamics* and *nozzle performance*, alone and in combination, in controlling the amount of soot produced, and (*ii*) the requirement for spatially resolved, nonintrusive optical measurements in order to guide combustor design, nozzle design, and fuel property specifications for future fuels.
- To unravel and delineate the coupling between the aerodynamics and nozzle performance, and for the results derived from nonintrusive optical measurements in aerodynamically complex flows to be of quantitative as well as qualitative value:
  - -Optical techniques must be pursued to extend the resolvable size to encompass sizes below 0.05 μm.
  - -Spatially resolved measurements of the velocity and temperature must be acquired to facilitate interpretation of the soot field data.

Acknowledgments

The results presented were obtained in a soot formation/alternative fuels study in progress at the UCI Combustion Laboratory and supported by the Air Force Engineering and Service Center, Research and Development Directorate, Environics Division (Air Force Contract FO-8635-83-C-0052) with Captain Paul Kerch as the project manager. The authors gratefully acknowledge (*i*) the assistance of Roger Rudoff and Randy Smith in the collection, reduction, and presentation of the data, (*ii*) the assistance of Tom Jackson and Robyn Charles for their work in the spray analysis of the Parker-Hannifin twin-fluid injector, (*iii*) the cooperation of Parker-Hannifin in the provision of the nozzle and the valuable technical discussions with Mr. Harold Simmons and Mr. Curt Harding, and (*iv*) the kindness of KVB Engineering and Dr. Larry Muzio for providing use of the Malvern droplet analyzer. The optical particulate measurement system was developed under subcontract to Spectron Development Laboratories, with Dr. Chie Poon serving as the principal in the design.

References

1 Churchill, A. V., DeLaney, C. L., and Lander, H. R., "Future Aviation Turbine Fuels," *J. Aircraft*, Vol. 15, No. 11, 1978, pp. 731–734.

2 Prado, G. P., Lee, M. L., Hites, R. A., Hoult, D. P., and Howard, J. B., "Soot and Hydrocarbon Formation in a Turbulent Diffusion Flame," *Sixteenth Symposium (International) on Combustion*, The Combustion Institute, 1976, pp. 649–661.

3 Wyatt, W. R., Clark, J. A., Peters, J. E., and Mellor, A. M., "Size Distribution and Surface Area Measurements of Gas Turbine Combustor Smoke," *Journal of Energy*, Vol. 3, No. 5, 1979, pp. 285–290.

4 Himes, R. M., Hack, R. L., and Samuelsen, G. S., "Chemical and Physical Properties of Soot as a Function of Fuel Molecular Structure in a Swirl-Stabilized Combustor," ASME JOURNAL OF ENGINEERING FOR GAS TURBINES AND POWER, Vol. 106, No. 1, Jan. 1984, pp. 103–108.

5 Hack, R. L., Samuelsen, G. S., Poon, C. C., and Bachalo, W. D., "An Exploratory Study of Soot Sample Integrity and Probe Perturbation in a Swirl-Stabilized Combustor," ASME JOURNAL OF ENGINEERING FOR POWER, Vol. 103, No. 10, 1981, pp. 759–771.

6 Samuelsen, G. S., Wood, C. P., and Jackson, T. A., "Optical Measurements of Soot Size and Number Density in a Complex Flow, Swirl-Stabilized Combustor," Combustion Problems in Turbine Engines, AGARD Conference Proceedings, No. 353, North Atlantic Treaty Organization, Oct. 1983.

7 Brum, R. D., and Samuelsen, G. S., "Assessment of a Dilute Swirl Combustor as a Bench Scale, Complex Flow Test Bed for Modeling, Diagnostics, and Fuels Effects Studies," AIAA Paper No. 82-1263, 1982.

8 Brum, R. D., and Samuelsen, G. S., "Two-Component Laser Anemometry Measurements in a Nonreacting and Reacting Complex Flow Model Combustor," WSS/CI Paper 82-53, 1982.

9 Parker-Hannifin. private communication by Mr. Curt Harding, 1983.

10 Sawyer, R. F., "Experimental Studies of Chemical Processes in a Model Gas Turbine Combustor," *Emissions From Continuous Combustion Systems*, edited by W. Cornelius and W. G. Agnew, Plenum, New York, 1972, pp. 243–254.

11 Fenton, D. L., Luebcke, E. H., and Norstrom, E., "Physical Characterization of Particulate Material From a Turbine Engine," ASME Paper 79-GT-179, 1979.